

# Preparation of Nanochitosan as an Effective Adsorbent for Removal of Pb (II) From Aqueous Solution

Camellia Zareie<sup>1</sup>, Saeideh Kholghi Eshkalak<sup>2</sup>, Ghasem Najafpour Darzi<sup>3\*</sup>, Mazyar Sharifzadeh baei<sup>4</sup>, Habibollah Younesi<sup>5</sup>, Seeram Ramakrishna<sup>6\*</sup>

<sup>1</sup> Department of Chemical Engineering, Faculty of Chemical Engineering, Tarbiat Modares University, P.O. Box: 14115-114, Tehran, Iran.

<sup>2</sup> Department of Polymer Engineering and Color Technology, Amirkabir University of Technology, 424 Hafez Ave, 15875-4413, Tehran, Iran.

<sup>3</sup> Faculty of Chemical Engineering, Babol Noshirvani University of Technology, Shariati Avenue, Babol, Iran

<sup>4</sup> Department of Chemical Engineering, Sciences and Research Ayatollah Amoli branch of Islamic Azad University, Amol, Iran

<sup>5</sup> Department of Environmental Science, Faculty of Natural Resources, Tarbiat Modares University, Noor, Iran.

<sup>6</sup> Department of Mechanical Engineering, Center for Nanofibers & Nanotechnology, Faculty of Engineering, National University of Singapore, Singapore 117576

\*Corresponding authors email address: [najafpour@nit.ac.ir](mailto:najafpour@nit.ac.ir) , [seeram@nus.edu.sg](mailto:seeram@nus.edu.sg)

## Abstract

In this work, nanochitosan (NC) was prepared through ionic gelation using low-molecular-weight chitosan and maleic acid (MA). The synthesized NC was characterized by means of Fourier Transform Infrared Spectroscopy (FTIR), Atomic Force Microscopy (AFM) and Scanning Electron Microscopy (SEM). In the course of preparation, the particle size of the material was strongly depended on the parameters such as chitosan concentration and pH of the solution. By controlling the above parameters, NC with the size of smaller than 100 nm was prepared. The chitosan and prepared NC were used for the adsorption of Pb (II) from aqueous solutions in a batch system. Among the sorption parameters, pH showed the strongest effect on the sorption process and maximum Pb (II) removal was obtained at pH value of 6. The pseudo-first-order and pseudo-second-order were used to track the kinetics of adsorption process. Langmuir and Freundlich isotherms were subjected to sorption data to estimate the sorption capacity. NC proved to be an excellent adsorbent with remarkable capacity to remove Pb (II) ions from the aqueous solutions at various concentrations. The NC also showed incredible performance with a comparatively easier preparation process than other reported work.

**Keywords:** Adsorption; Chitosan; Isotherm; Nanochitosan; Pb (II) removal

## 1. Introduction

Heavy metals Pollution is considered as a serious threat for the environment and public health due to their non-biodegradability, toxicity, and bioaccumulation in organisms [1]. Generally, heavy metals are very toxic, can cause serious damages in living organism even at low concentrations [2]. Pb (II), a heavy metal, can cause irreversible damages to brain, the nervous and kidney systems following entry in human body. These damages may cause cancer,

amnesia and mental retardation [3]. Due to high toxicity of Pb (II), the United States Environmental Protection Agency (USEPA) has set a very low tolerance limit of Pb (II) (0.015 mg/L) for drinking water [4]. Various techniques are used for the removal of heavy metals from water and wastewater including chemical precipitation [5], ion-exchange [6], membrane [7] and adsorption [8-11]. Adsorption, among them, is appealing due to easy application, low cost and remarkable efficiency. This has made it a centre of attention for synthesis and preparation of novel and efficient adsorbents in recent decades [2]. Various types of adsorbents such as activated carbon [6], nanotube [9] and bentonite [10], have been widely used for the removal of Pb(II) from water and wastewater.

Chitosan as a linear polysaccharide includes randomly distributed  $\beta$ -(1 $\rightarrow$ 4)-linked D-glucosamine (deacetylated unit) and N-acetyl-D-glucosamine. It is commonly produced by the reaction of the chitin (obtained from shells of shrimp and other crustaceans) with an alkaline substance (commonly sodium hydroxide) [12]. Chitin is insoluble in aqueous solutions but soluble in acidic solutions owing to the free protonable amine groups in its structure [13]. Recent widespread application of chitosan for the removal of metal ions from aqueous media is due to the existence of hydroxyl and amine groups in their chemical structure, having high potential to bind with metal ions [4, 14]. Excessive sensitivity of chitosan to pH can make it in form of gel or dissolved at various pH values [15]. In order to overcome such challenge, cross-linked chitosan instead of conventional untreated chitosan [4, 16] such as glyoxal, formaldehyde, glutaraldehyde and isocyanates [17-19] is used. Some of cross-linked chitosan have been used as adsorbents for the removal of metal ions from water and wastewater. For instance, Kyzas et al. [20] synthesized two novel cross-linked chitosan and used them for the adsorption of Cd<sup>2+</sup> and Pb<sup>2+</sup>; resulted in considerably improved adsorption capacity after cross-linking. The cross-linked magnetic chitosan has also been prepared and used for adsorption of Pb<sup>2+</sup> from aqueous solution [2].

In this work, preparation of nanochitosan (NC) by addition of  $K_2S_2O_8$  as the cross-linking agent into a chitosan solution was performed. The primary aim was to produce NC with the size of less than 100 nm to be used in various fields. In order to investigate the effect of experimental conditions on nanoparticles size and aggregation, the samples were characterized with advanced techniques such as Fourier transform infrared spectroscopy (FT-IR), scanning electron microscopy (SEM) and Atomic Force Microscopy (AFM). The second purpose of this study was to remove Pb (II) ions from aqueous solution by NC in a batch system. The effect of pH, NC dosage and contact time on adsorption of metal ions were investigated. Adsorption isotherms and kinetics were also studied.

## 2. Material and Methods

### 2.1. Materials

Chitosan (MW= 50 ~ 190 kDa), with a degree of acetylation of (75 ~ 85 %) was purchased from Sigma-Aldrich. Maleic acid (MA) and lead nitrate were purchased from Merck (Darmstadt, Germany).

### 2.2. Preparation of NC

NC was prepared according to a developed method by de Moura et al. [21]. Initially, chitosan and MA were dissolved in distilled water, stirred for 30 min by magnetic stirrer (VELP, SCIENTIFICA, Europe) at 300 rpm. Subsequently, 0.2 mmol of  $K_2S_2O_8$  was added to the solution under continuous stirring at 70°C for 7 h; followed by cooling the mixture in an ice bath until a milky emulsion was obtained. The suspension was centrifuged for 15 min at 16000 rpm and then placed in a freeze dryer [22]. Figs. 1 and 2 depict the maleic acid polymerization mechanism and chitosan -MA nanoparticle formation.

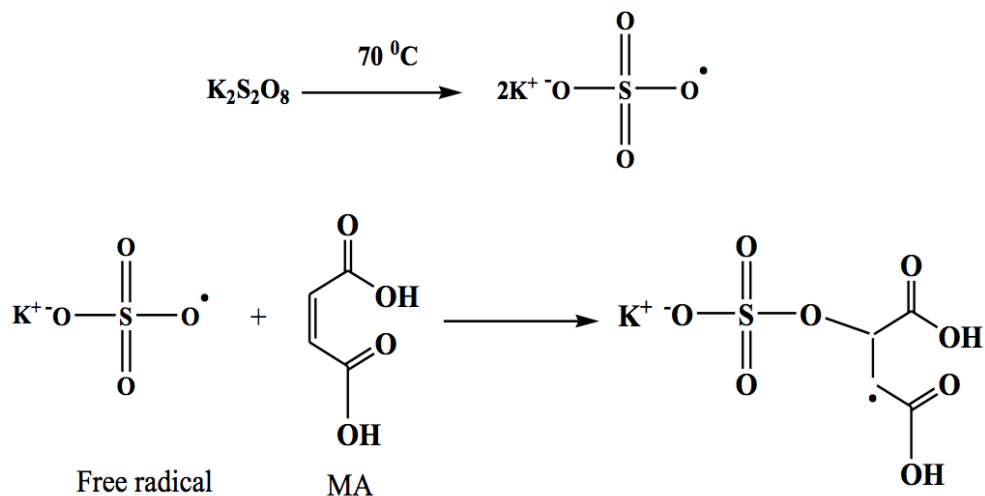


**Fig. 1.** Schematic maleic acid polymerization mechanism

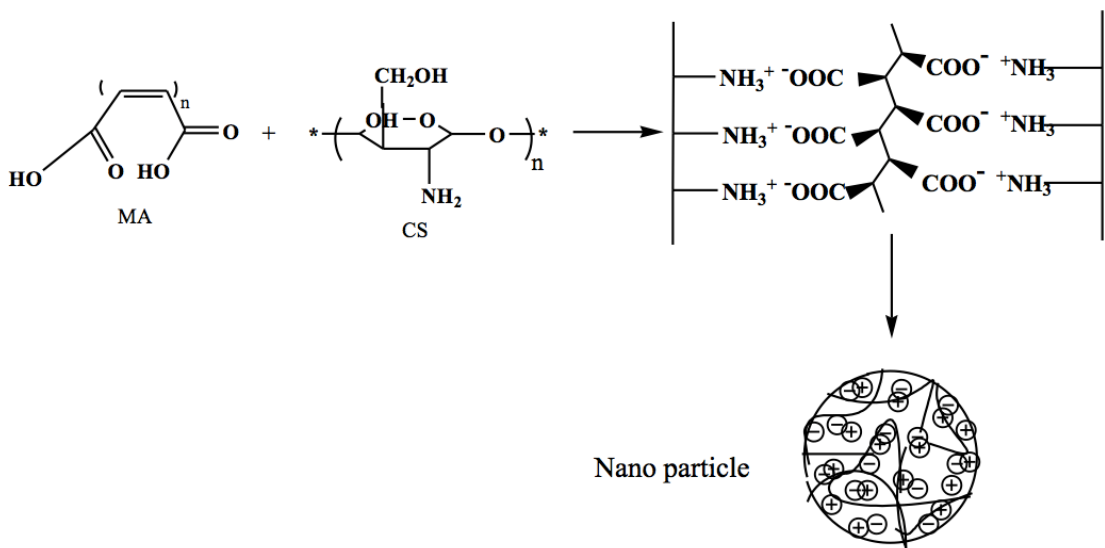


**Fig. 2.** Schematic of chitosan-MA nanoparticle formation

### 2.3. Characterizations of chitosan and NC

The surface morphologies of chitosan and NC samples were analysed by using Scanning Electron Microscopy (SEM) KYKY model EM3200 microscope. For the SEM analysis, the sample was placed in a vacuum and operated at a typical accelerating voltage of 25 kV.

Chitosan and NC were analysed by a Shimadzu Spectrum model 8400s FTIR spectra in the range of 4000 to 400  $\text{cm}^{-1}$ . A SensAA atomic absorption spectrometer (from GBC scientific equipment, Australia), equipped with a lead hollow cathode lamp was used for determination of Pb (II) concentration in the aqueous media.

## 2.4. Batch experiment

All experiments for adsorption of Pb (II) ions on chitosan and NC adsorbent were carried out in a batch system at room temperature (25 °C). The pH of solution was adjusted by adding 1N HCl and 1M NaOH solutions. In all of the above experiments, the amount of metal ions adsorbed was calculated according to following equation:

$$q_e = (C_0 - C_e) \times \frac{V}{m} \quad (1)$$

where  $q$  is the amount (mg/g) of metal ions adsorbed by NC, chitosan;  $C_0$  and  $C_e$  (mg/L) are the initial and final metal concentrations in the solution, respectively;  $V$  (L) is the volume of the solution and  $m$  (g) is the mass of (dry) adsorbent used. The removal efficiency calculated as follows:

$$R = \frac{C_0 - C_f}{C_0} \times 100 \quad (2)$$

## 3. Results and Discussion

### 3.1. Synthesis of Nanochitosan

Wen Fan et al., [23] found that the formation of chitosan nanoparticles to be depended on the concentration of chitosan solution, mass ratio of chitosan to cross-linking agent and pH of chitosan solution. Hence, to avoid the formation of micro-particles, the synthesis parameters such as the concentration of chitosan, the concentration of cross-linking agent and pH of the solution should be adjusted. The morphology of the prepared NC samples in various ranges of

chitosan concentrations and pH of the solution was evaluated by SEM. In this study, the pH of solution was adjusted in the range of 3 to 6 and mass ratio of chitosan/MA was 2:1 and 1:1. In the acid solution, the amine groups of chitosan and carboxyl groups of MA were protonated with possible influence on the size of nanoparticles. Figs. 1 and 2 show a typical schematic of chitosan-MA nanoparticles formation. It depicts the electrostatic interactions of MA- chitosan resulted in the formation of nanoparticles through the polymerization of MA in presence of chitosan molecules. At a certain level of MA polymerization, the formation of chitosan-MA nanoparticles occur with linkages between negative charged MA carboxyl groups and chitosan amine groups.

As shown in Fig. 3, the mass ratio of chitosan/MA affect the shape and structure of NC remarkably. At the chitosan/MA mass ratio of 1:1, the ratio of  $\text{NH}_2/\text{COOH}$  is 0.5. As seen, due to higher ratio of MA acid functional group compared to chitosan functional group at this mass ratio, the polymerization of MA (instead of NC production) and subsequently, extensive aggregation of products is observed. The NC are produced by the binding between the carboxyl group of MA and protonated amine group of chitosan. When the ratio of the functional group of chitosan is higher than or equal to MA, the whole amount of MA contributes in the reaction with the amine functional group of chitosan. The main purpose of this study was to synthesize the NC from chitosan and application of NC for the removal of Pb (II) from aqueous solution. Therefore, for production of NC, the chitosan/MA a mass ratio of 2:1 was selected. As shown in Fig. 3, the nanoparticles size increases by increasing pH from 3 to 6. There are two reasons for this behaviour: firstly, increasing pH of solution may also lead to increase degrees of ionization and charge density of MA molecules. Hence, the repulsive electrostatic forces of internal MA molecules rise, cause inflation in nanoparticles and as a result increase the size of particles. Secondly, the reduction in solubility of chitosan by increasing pH, may increase the

adhesion and aggregation of nanoparticles. The results are indicative of an increase in the particle size by increasing the concentration of chitosan.

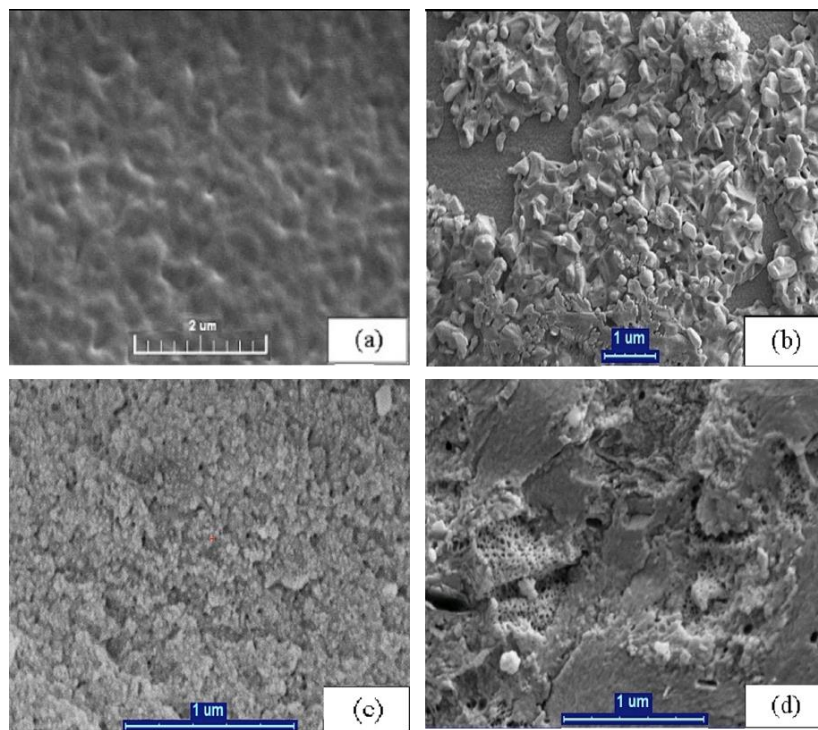


**Fig. 3** SEM of nanochitosan in mass ratio of chitosan/MA=1 and at several pH (a) pH=3, (b) pH=4, (c) pH=5, (d) pH=6

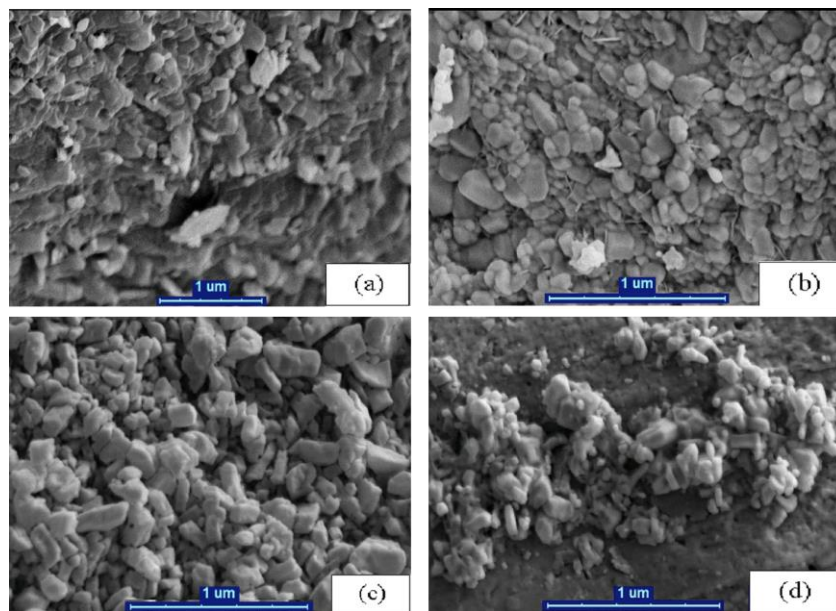


**Fig. 4** SEM of nanochitosan in mass ratio of chitosan/MA=2 and at several pH (a) pH=3, (b) pH=4, (c) pH=5, (d) pH=6

The SEM image of chitosan is shown in Fig. 5. Chitosan presents a nonporous and smooth morphology; whereas the SEM image of NC exhibits a porous and chain-like morphology. d

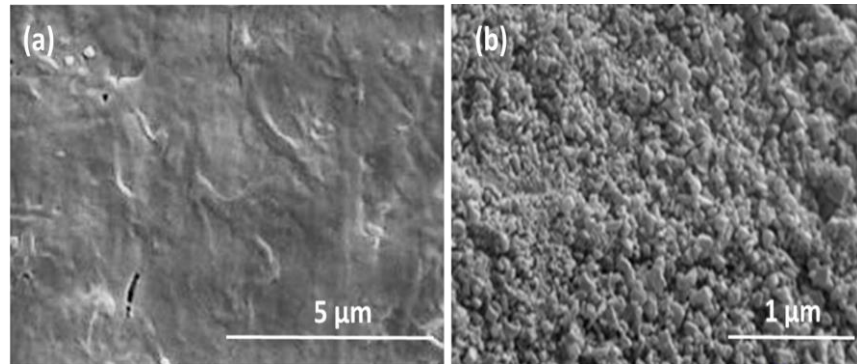


**Fig. 5** SEM of (a) Chitosan and (b) NC (mass ratio of chitosan/MA= 2:1, pH=4)

It seems that increasing the mass ratio of chitosan helped to increase the diameter of NC, to above 180 nm (Figs. 6 and 7). Since all of MA molecules were used in the production of nanoparticles, extra chitosan molecules may increase the diameter of nanoparticles. The best result was obtained at pH=4 and a mass ratio of chitosan/MA=2.

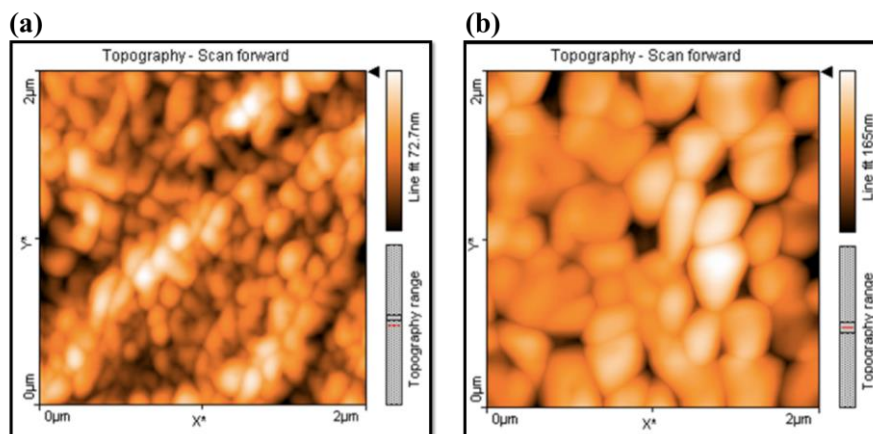


**Fig. 6** AFM images of NC (a) Mass ratio of chitosan/MA= 2:1, pH=4, (b) pH=5

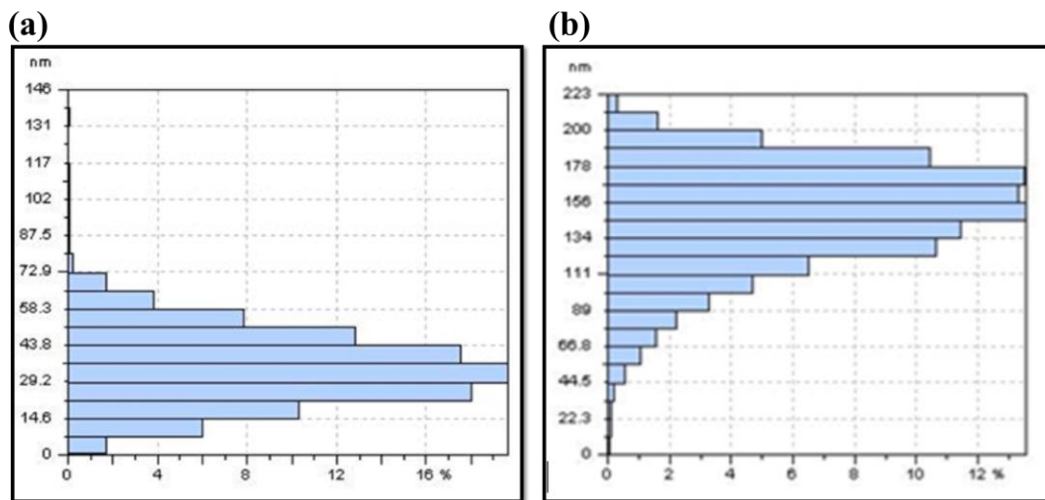


**Fig. 7** Nanochitosan size distribution (a) Mass ratio of chitosan/MA= 2:1, pH=4, (b) pH=5

At the end of the production process, colloidal suspensions opalescence, as a confirmation of the end of the process, was observed. Fig. 8 clearly shows good stability of nanoparticles in suspension after 22 days confirming the suspension's applicability in different fields, namely pharmacy (need solution instead of solid particles). It is interesting to observe that the nanoparticles were formed spontaneously without a need for high temperature treatment or application of organic solvents.

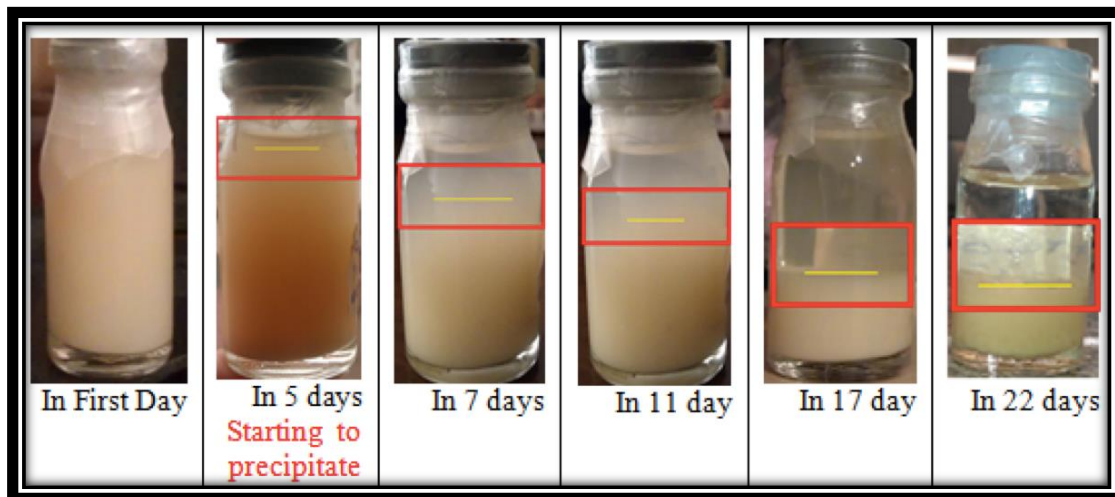


**Fig. 8** Stability of chitosan-MA nanoparticle solution (mass ratio 1:1, pH=4)

Fig. 9 displays an FT-IR spectrum of NC with various functional groups. The chitosan spectrum presents a characteristic peak at  $3435\text{ cm}^{-1}$  corresponding to the stretching vibration of  $\text{NH}_2$  and  $\text{OH}$  groups; whereas the bands at  $1660$  and  $3050\text{ cm}^{-1}$  correspond to  $\text{N-H}$  and the  $\text{NH}_2$  groups; the one at  $1700\text{ cm}^{-1}$  is associated with  $\text{C=O}$  and that at  $1080\text{ cm}^{-1}$  corresponds to the  $\text{C-O}$  stretching vibration. Presence of two new bands at  $1638$  and  $1545\text{ cm}^{-1}$ , corresponding to  $\text{COO}^-$  and  $\text{NH}^{+3}$  groups, respectively, were observed. These indicate ionic interaction between MA and chitosan associated with the formation of NC [24]. The bands at  $1700$  and  $1600\text{ cm}^{-1}$ , corresponding to  $\text{C=O}$  and  $(\text{C-C})$  confirm the presence of MA in the nanoparticles' compositions.

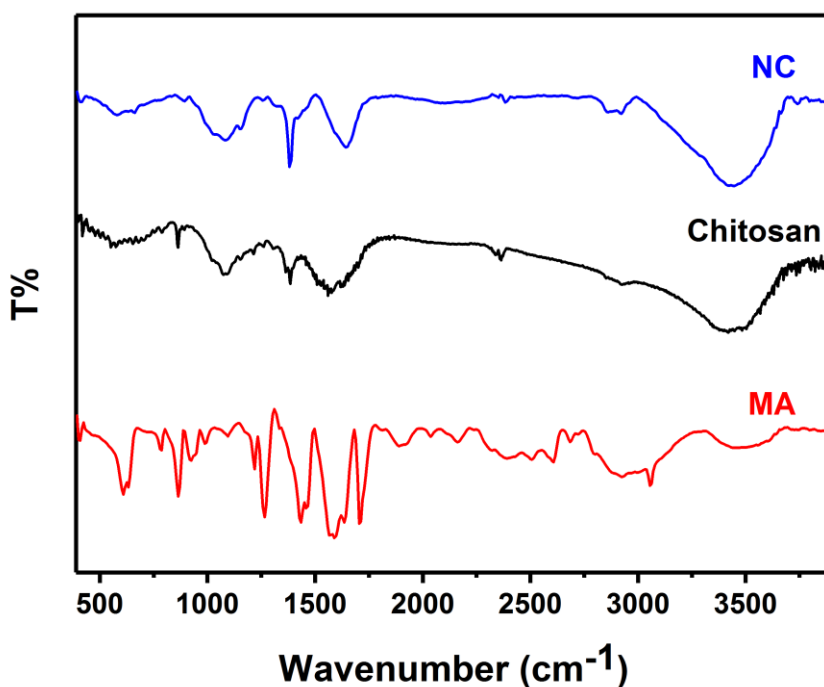


**Fig. 9** FTIR spectra of Maleic acid, chitosan, and NC

### 3.2. Adsorption of Pb (II) from aqueous solution by chitosan and NC

#### 3.2.1. Effect of pH

The pH of a solution plays an important role in adsorption processes as it can influence the chemical structure of metal ions and active sites of adsorbents [25]. Fig. 10 shows the effect of pH (4 to 6) on the adsorption of Pb (II) ions by NC and chitosan. The removal efficiency increased sharply with increasing pH up to 6. Above pH of 6.0, Pb (II) ions precipitated in the form of hydroxide. At pH of 6, the removal efficiency of Pb (II) ions for NC and chitosan were 93.88 and 66.32%, respectively. At pH less than 4, the adsorption rate was very low since the adsorbent surface was entirely covered with  $H^+$  that competed strongly with Pb (II) ions for adsorption sites, hence minimized the possibility of Pb (II) adsorption [26]. In the range of  $4 < pH < 6$ , the  $H^+$  ions concentration decreased and Pb (II) ions had higher chance to be adsorbed on the active sites of NCS or Cs. Hence, the optimum pH for the adsorption of Pb (II) ions was defined to be 6; thus, this pH was selected for all other experiments in this work.

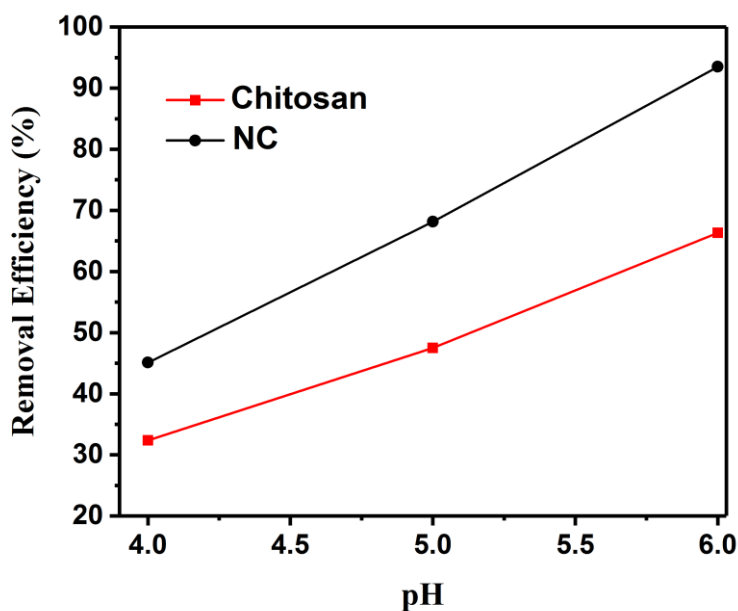


**Fig. 10** Effect of contact time on the removal efficiency of Pb (II) ions by NC and chitosan. (initial concentration 10 mg/L, adsorbent mass 2.5 g/ L, shaking rate 180 rpm, temperature 298 K)

### 3.2.2. Effect of contact time

The removal efficiency of Pb (II) ions by chitosan and NC is shown in Fig. 11. The results indicated that adsorption process had two stages, firstly the initial rapid adsorption stage accounting for a large part of total adsorption. The removal rate was high and majority of Pb (II) ions were adsorbed in the first 30 minutes. The second stage had a smaller share of adsorption in which the adsorption process was slow, and the equilibrium was observed in less than 1 and 1.5 h for NC and chitosan, respectively. Therefore, for further experiments, the contact times were selected to be 60 min and 90 min for NC and chitosan, respectively. Though, it had been reported that long time was required for lead sorption from aqueous solutions by chitosan [27]; in contrast, in this research, the removal of Pb (II) ions from aqueous solutions was obtained in a short contact time. This was attributed to the large surface area and high surface reactivity of NC. The results also indicated that the Pb (II) adsorption capacity of NC was superior than the chitosan.

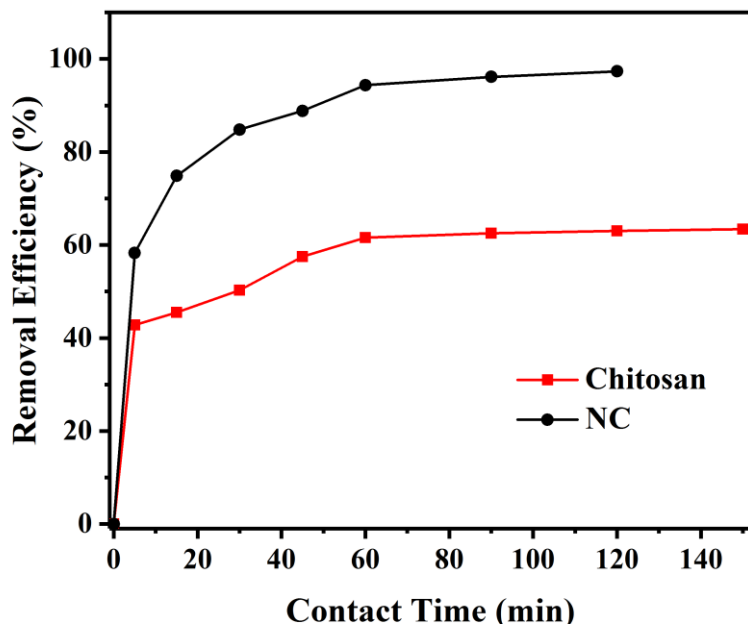


**Fig. 11** Effect of contact time on the removal efficiency of Pb (II) ions by NC and chitosan. (initial concentration 10 mg/L, adsorbent mass 2.5 g/L, shaking rate 180 rpm, temperature 298 K)

### 3.2.3. Adsorption Kinetics

The adsorption kinetics provides important information about the reaction paths and the rate of the process. To determine the controlling mechanism for the adsorption process, both pseudo-first-order (Eq. 3) and pseudo-second-order (Eq. 4) kinetic models were used [28, 29].

$$\log(q_e - q_t) = \log q_e - \frac{k_1}{2.303} t \quad (3)$$

$$\frac{t}{q_t} = \frac{1}{k_2 q_e^2} + \frac{t}{q_e} \quad (4)$$

where  $q_t$  (mg/g) is the amount of metal ion adsorbed at contact time  $t$  (min);  $q_e$  (mg/g) is the adsorption capacity at adsorption equilibrium; and  $k_1$  ( $\text{min}^{-1}$ ) and  $k_2$  (g/ mg.min) are the kinetic rate constants for the pseudo first order and the pseudo second order models, respectively.

In the present investigation, the adsorption data were utilized to examine the amount of Pb (II) ions adsorbed as a function of contact time, for initial metal ions concentrations in the range of 10 to 100 mg/L. The removal of Pb (II) ions increased with the contact time and the system reached equilibrium after 60 min for NC and 90 min for chitosan. Increasing the concentration of metal ions in the solution, increased the chance of effective collision between the metal ions and the adsorbent and resulted in improved metal ions removal.

The kinetic adsorption of Pb (II) ions was fitted to Eqs. (3) and (4), and the calculated data are presented in Table 1. A comparison between the observed and the calculated values of  $q_t$ , against time revealed a very good fit with the pseudo-second-order rate equation compared that with the pseudo first order rate equation for both adsorbents. Therefore, the adsorption of lead ions is well represented by the pseudo second order kinetic model (Figs. 12 and 13). The pseudo second order rate constants are slightly different for the five initial Pb (II) ions concentrations, reflection the inferior effect of initial concentration. Adoption of pseudo-second order kinetic model means that the rate-limiting step might be chemisorption's involving valence forces through sharing or exchanging electrons between adsorbent and

adsorbate [30]. Azizian demonstrated that the adsorption process obeyed first-order kinetics at high initial concentration of pollutants whereas it followed a pseudo-second-order kinetics at lower initial concentration of pollutants [31, 32].

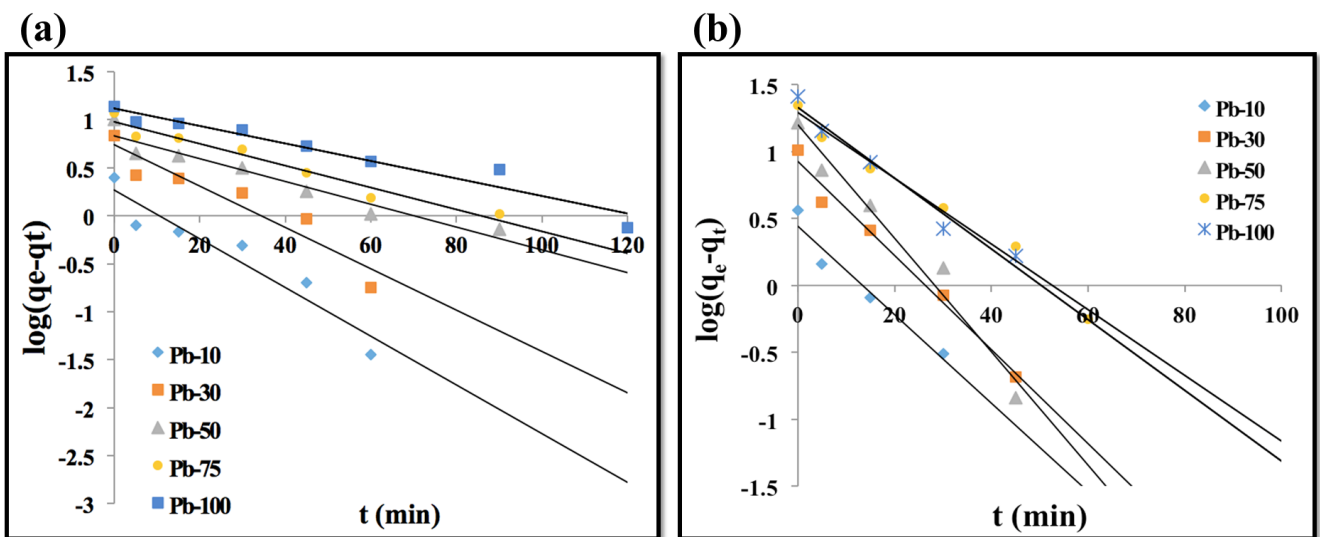


**Fig. 12** Pseudo first order model of a) Chitosan and b) NC for Pb (II) ions (pH =6, adsorbent mass 2.5 g/L, shaking rate 180 rpm, temperature 298 K)

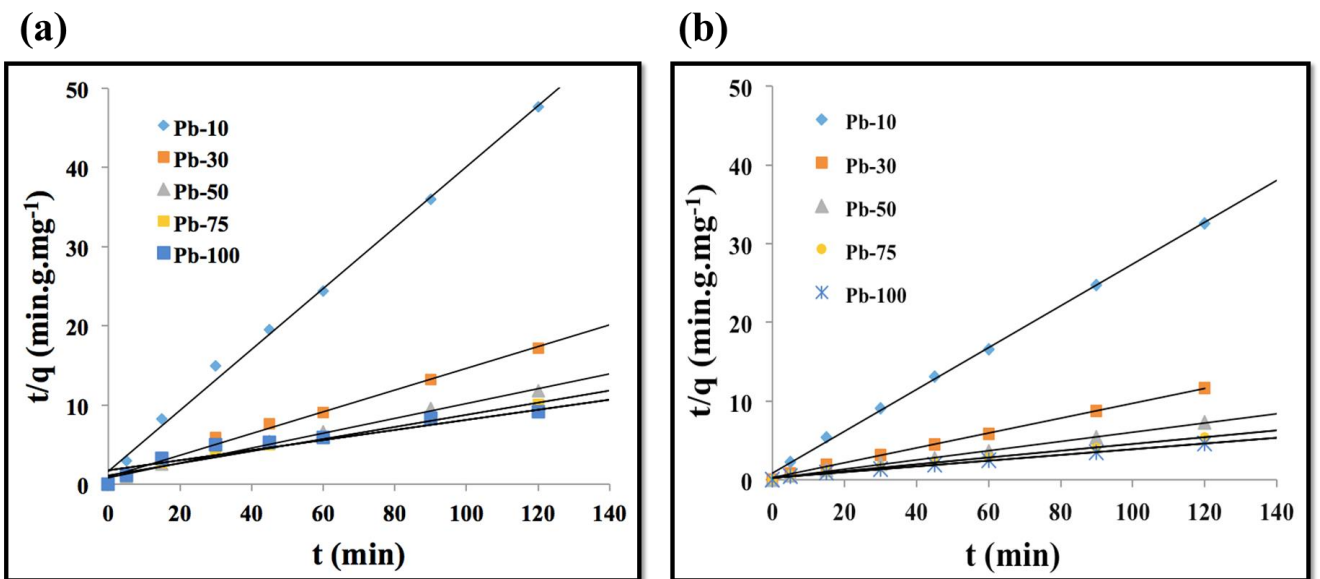


**Fig. 13** Pseudo-second order model of a) Chitosan and b) NC for Pb (II) ions (pH =6, adsorbent mass 2.5 g/L, shaking rate 180 rpm, temperature 298 K).

**Table 1** Adsorption kinetic parameters of Pb ions using chitosan and NCS

Sorbent	Initial Pb conc. (mg/l)	q <sub>e</sub> , exp (mg/g)	Pseudo first order			Pseudo second order		
			k <sub>1</sub> (min <sup>-1</sup> )	q <sub>e1</sub> (mg/g)	R <sup>2</sup>	k <sub>2</sub> (g·mg <sup>-1</sup> ·min <sup>-1</sup> )	q <sub>e2</sub> (mg/g)	R <sup>2</sup>
Chitosan	10	2.50	0.0576	1.894	0.908	0.0905	2.60	0.997
	30	6.83	0.0484	5.483	0.932	0.0207	7.30	0.994
	50	10.15	0.0253	6.792	0.930	0.0992	10.87	0.994
	75	11.88	0.0258	9.528	0.957	0.0521	13.16	0.986
	100	12.60	0.0207	13.122	0.938	0.0226	15.87	0.975
NCS	10	3.62	0.0759	2.761	0.949	0.0833	3.77	0.998
	30	10.26	0.0806	8.414	0.984	0.0322	10.64	0.998
	50	16.45	0.0956	15.78	0.969	0.0192	17.24	0.998
	75	22.12	0.0553	19.498	0.984	0.0752	23.26	0.997
	100	25.82	0.0598	21.281	0.971	0.0525	27.78	0.996

### 3.2.4. Adsorption Isotherms

Adsorption isotherm model is essential in order to predict and compare the performance of adsorbents. Equilibrium studies described the affinity and surface properties of adsorbents by constant values and characterize the adsorption capacity of adsorbents [38]. The adsorption isotherms, Langmuir and Freundlich were studied at different initial metal ions concentrations in the range of 10–100 mg/ L on NC and chitosan (Figs. 14 and 15). The expressions of Langmuir isotherm and linear form of this isotherm are presented in Eqs. (5) and (6).

$$q_e = \frac{q_m k_L C_e}{1 + k_L C_e} \quad (5)$$

$$\frac{C_e}{q_e} = \frac{1}{k_L q_m} + \frac{C_e}{q_m} \quad (6)$$

where  $q_e$  and  $C_e$  are the adsorption capacity (mg/g) and the equilibrium concentration of the adsorbate (mg/L), respectively, while  $q_m$  represents the maximum adsorption capacity of adsorbents (mg/g).  $K_L$  is the Langmuir constant (L/mg) representing the affinity of binding sites and is a measure of the energy of adsorption. Langmuir isotherm assumes that the maximum adsorption capacity occurs on a monolayer of adsorbent surface. This model expresses that all the adsorption sites of adsorbent has an equal energy and the intermolecular forces decrease when the distance from the surface of adsorption increases.

Freundlich isotherm model assumes that adsorption occurs at multilayers and various sites of adsorbent have different energies. Eqs. 7 and 8 show Freundlich isotherm model and its linear form:

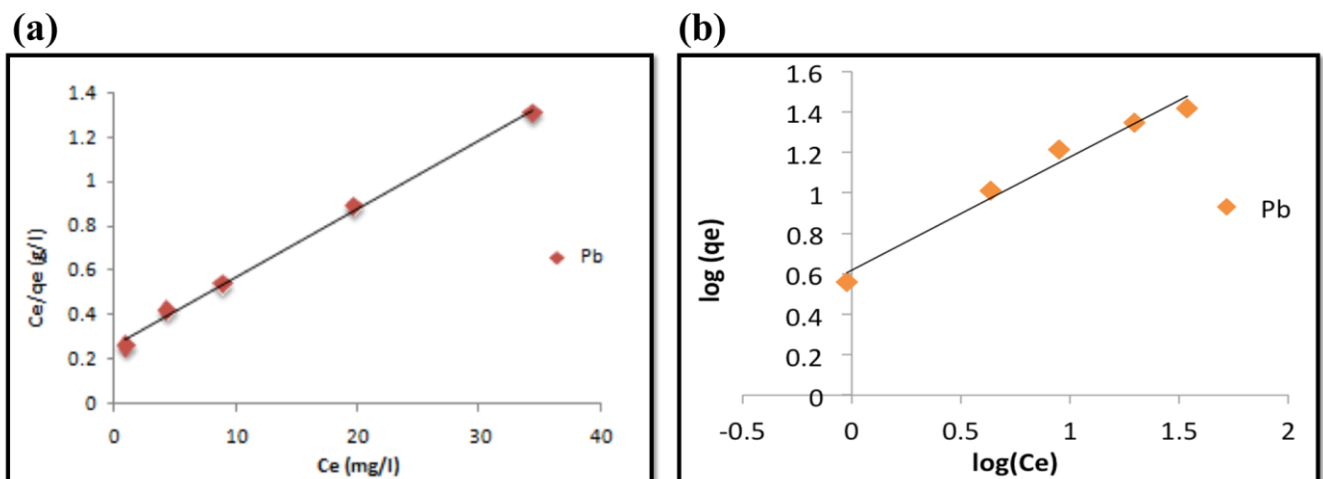
$$q_e = k_F C_e^{\frac{1}{n}} \quad (7)$$

$$\ln q_e = \ln k_F + \frac{1}{n} \ln C_e \quad (8)$$

the  $n$  and  $K_F$  (mg/g) are Freundlich constants related to the adsorption intensity and adsorption capacity. Fig. 14 presents (a) Langmuir and (b) Freundlich linear fittings, respectively; whereas the isotherms constants are presented in Table 2. Based on the regression factor ( $R^2$ ), the Langmuir model defined the experimental data better than Freundlich model for both NC and chitosan, implying the predominant occurrence of the monolayer adsorption. Langmuir isotherm well fit to the experimental data may also be owing to the homogenous distribution of active sites on the NC and chitosan (Langmuir equation assumes that the surface is homogenous) [39]. The maximum adsorption capacity ( $q_m$ ) obtained from the Langmuir isotherm was 32.26 mg/g. The magnitude of the exponent  $n$  shows the favourability of adsorption;  $n > 1$  and  $n < 1$  represent good and poor adsorption characteristics, respectively. Freundlich and Langmuir adsorption isotherms generally indicate the surface heterogeneity and homogeneity, respectively.

**Table 2.** The parameters of isotherm models for *Pb* adsorption

Adsorbent	Langmuir isotherm			Freundlich isotherm		
	$q_m$	$k_L$ (l/mg)	$R^2$	$n$	$k_F$	$R^2$
NCS	32.26	0.1188	0.997	1.790	4.140	0.975
chitosan	16.39	0.055	0.991	1.78	1.422	0.905

**Fig. 14.** a) Langmuir isotherm plot, b) Freundlich isotherm plot for the adsorption of Pb (II) ions on NC.

### 3.3. Comparison of NCS adsorption capacity with other adsorbents

In order to have a better understanding about the adsorption capacity of NC, the obtained experimental results were compared with several adsorbents, such as chitosan-pectin pellets, chitosan crosslinked with ECH, procion green H-4G immobilized pHEMA/chitosan, crosslinked carboxymethyl-chitosan resin, pristine chitosan and copolymer 2-hydroxyethyl methacrylate with monomer methyl methacrylate. Table 3 shows the experimental results of several adsorbents based on the adsorption capacity. As can be seen, the adsorption capacity of the synthesized NC in this study was much better than adsorbents such as chitosan chitosan-pectin pellets, Crosslinked carboxymethyl-chitosan resin and Pristine Chitosan. However, NC showed inferior adsorption capacity to Chitosan crosslinked with ECH and Procion Green H-4G immobilized pHEMA/chitosan. It should be mentioned that the NC, in this study, was

synthesized by a simple and easy process; whereas the synthesis procedures of chitosan crosslinked with ECH or Procion Green H-4G immobilized pHEMA/chitosan are not simple.

**Table 3.** Comparison between NCS and other adsorbents.

Adsorbent	Pb (II) $q_e$ , mg/g	Refs.
Chitosan	13.1	mg/g (Chen et al. 2008)
Chitosan–pectin pellets	11.9	mg/g (Debbaudt, Ferreira and Gschaider 2004)
Chitosan crosslinked with ECH	34.13	mg/g (Chen et al. 2008)
Procion Green H-4G immobilized pHEMA/chitosan	68.81	mg/g (Genç et al. 2003)
Crosslinked carboxymethyl-chitosan resin	0.15	mmol/g (Sun, Wang and Wang 2006)
Copolymer 2-hydroxyethyl methacrylate with monomer methyl methacrylate	31.5	mg/g (Moradi et al. 2009)
NCS	32.26	mg/g This study

## 4. Conclusions

NC was successfully prepared by polymerizing MA in the presence of CS solution. The particle size is highly dependent on the chitosan concentration used in preparation method and is greatly influenced by the pH of the solution. SEM and AFM analyses show that chitosan nanoparticles have a very homogeneous morphology and quite uniform particles size distribution. The capacity of NC application for the removal of Pb (II) from aqueous solution was also investigated. The study strongly recommended that NCs can be introduced as a suitable adsorbent for the removal of Pb (II) from the aqueous solution. The maximum Pb (II) ions adsorption capacity of NC was very close to other reported chitosan, and superior to some

of them. The optimum conditions of sorption by NC were found to be: the contact time of 60 min and pH of 6 for Pb(II). The obtained results from this work were well fitted by the theoretical Freundlich isotherm. The kinetic data showed that the adsorption process controlling was performed by a pseudo-second-order equation.

## Acknowledgements

The authors wish to acknowledge Babol Noshirvani University of Technology, Biotechnology and Nano biotechnology research lab for the facilities provided to conduct present research.

## References

- [1] Shahzad A, Miran W, Rasool K, Nawaz M, Jang J, Lim S-R, et al. Heavy metals removal by EDTA-functionalized chitosan graphene oxide nanocomposites. *RSC Advances*. 2017;7:9764-71.
- [2] Shahraki S, Delarami HS. Magnetic chitosan-(d-glucosimine methyl) benzaldehyde Schiff base for Pb<sup>+</sup> 2 ion removal. Experimental and theoretical methods. *Carbohydrate polymers*. 2018;200:211-20.
- [3] Lu Z, Tan R, Chu W, Tang S, Xu W, Song W. Synthesis of SrHPO<sub>4</sub>/Fe<sub>3</sub>O<sub>4</sub> magnetic nanocomposite and its application on Pb<sup>2+</sup> removal from aqueous solutions. *Microchemical Journal*. 2018;142:152-8.
- [4] Yu Z, Dang Q, Liu C, Cha D, Zhang H, Zhu W, et al. Preparation and characterization of poly (maleic acid)-grafted cross-linked chitosan microspheres for Cd (II) adsorption. *Carbohydrate polymers*. 2017;172:28-39.
- [5] Rojas R. Copper, lead and cadmium removal by Ca Al layered double hydroxides. *Applied Clay Science*. 2014;87:254-9.
- [6] Dąbrowski A, Hubicki Z, Podkościelny P, Robens E. Selective removal of the heavy metal ions from waters and industrial wastewaters by ion-exchange method. *Chemosphere*. 2004;56:91-106.
- [7] Khulbe K, Matsuura T. Removal of heavy metals and pollutants by membrane adsorption techniques. *Applied water science*. 2018;8:19.
- [8] Vilela PB, Dalalibera A, Duminelli EC, Becegato VA, Paulino AT. Adsorption and removal of chromium (VI) contained in aqueous solutions using a chitosan-based hydrogel. *Environmental Science and Pollution Research*. 2018;1-9.

[9] Lin Y, Ma J, Liu W, Li Z, He K. Correction to: Efficient removal of dyes from dyeing wastewater by powder activated charcoal/titanate nanotube nanocomposites: adsorption and photoregeneration. *Environmental science and pollution research international*. 2019.

[10] Zou C, Jiang W, Liang J, Sun X, Guan Y. Removal of Pb (II) from aqueous solutions by adsorption on magnetic bentonite. *Environmental Science and Pollution Research*. 2019;26:1315-22.

[11] Liu Y, Luan J, Zhang C, Ke X, Zhang H. The adsorption behavior of multiple contaminants like heavy metal ions and p-nitrophenol on organic-modified montmorillonite. *Environmental Science and Pollution Research*. 2019;1-11.

[12] Rinaudo M. Chitin and chitosan: properties and applications. *Progress in polymer science*. 2006;31:603-32.

[13] Gutha Y, Munagapati VS. Removal of Pb (II) ions by using magnetic chitosan-4-((pyridin-2-ylimino) methyl) benzaldehyde Schiff's base. *International journal of biological macromolecules*. 2016;93:408-17.

[14] Liu B, Chen X, Zheng H, Wang Y, Sun Y, Zhao C, et al. Rapid and efficient removal of heavy metal and cationic dye by carboxylate-rich magnetic chitosan flocculants: Role of ionic groups. *Carbohydrate polymers*. 2018;181:327-36.

[15] Chiou M-S, Ho P-Y, Li H-Y. Adsorption of anionic dyes in acid solutions using chemically cross-linked chitosan beads. *Dyes and pigments*. 2004;60:69-84.

[16] Sutirman ZA, Sanagi MM, Karim JA, Naim AA, Ibrahim WAW. New crosslinked-chitosan graft poly (N-vinyl-2-pyrrolidone) for the removal of Cu (II) ions from aqueous solutions. *International journal of biological macromolecules*. 2018;107:891-7.

[17] Doshi B, Ayati A, Tanhaei B, Repo E, Sillanpää M. Partially carboxymethylated and partially cross-linked surface of chitosan versus the adsorptive removal of dyes and divalent metal ions. *Carbohydrate polymers*. 2018;197:586-97.

[18] Lu F, Astruc D. Nanomaterials for removal of toxic elements from water. *Coordination Chemistry Reviews*. 2018;356:147-64.

[19] Ngah WW, Teong L, Hanafiah MAKM. Adsorption of dyes and heavy metal ions by chitosan composites: A review. *Carbohydrate polymers*. 2011;83:1446-56.

[20] Kyzas GZ, Siafaka PI, Lambropoulou DA, Lazaridis NK, Bikaris DN. Poly (itaconic acid)-grafted chitosan adsorbents with different cross-linking for Pb (II) and Cd (II) uptake. *Langmuir*. 2014;30:120-31.

[21] Zolfaghari G, Esmaili-Sari A, Anbia M, Younesi H, Amirmahmoodi S, Ghafari-Nazari A. Taguchi optimization approach for Pb (II) and Hg (II) removal from aqueous solutions using modified mesoporous carbon. *Journal of hazardous materials*. 2011;192:1046-55.

[22] Zareie C, Najafpour G. Preparation of nanochitosan as an effective sorbent for the removal of copper ions from aqueous solutions. *International Journal of Engineering-Transactions B: Applications*. 2013;26:829-36.

[23] Fan W, Yan W, Xu Z, Ni H. Formation mechanism of monodisperse, low molecular weight chitosan nanoparticles by ionic gelation technique. *Colloids and Surfaces B: Biointerfaces*. 2012;90:21-7.

[24] de Moura MR, Aouada FA, Mattoso LH. Preparation of chitosan nanoparticles using methacrylic acid. *Journal of colloid and interface science*. 2008;321:477-83.

[25] Amini M, Younesi H, Bahramifar N, Lorestani AAZ, Ghorbani F, Daneshi A, et al. Application of response surface methodology for optimization of lead biosorption in an aqueous solution by *Aspergillus niger*. *Journal of hazardous materials*. 2008;154:694-702.

[26] Haider S, Park S-Y. Preparation of the electrospun chitosan nanofibers and their applications to the adsorption of Cu (II) and Pb (II) ions from an aqueous solution. *Journal of Membrane Science*. 2009;328:90-6.

[27] Zhang C, Li X, Pang J. Synthesis and adsorption properties of magnetic resin microbeads with amine and mercaptan as chelating groups. *Journal of applied polymer science*. 2001;82:1587-92.

[28] Lagergren S, Sevensk B. Zur theorie der sogenannten adsorption gelöster stoffe. *Vantens Kapsa Kedhandle*. 1898;24.

[29] Li G, Cai W, Zhao R, Hao L. Electrosorptive removal of salt ions from water by membrane capacitive deionization (MCDI): characterization, adsorption equilibrium, and kinetics. *Environmental Science and Pollution Research*. 2019;1-10.

[30] Javadian H, Ahmadi M, Ghiasvand M, Kahrizi S, Katal R. Removal of Cr (VI) by modified brown algae Sargassum bevanom from aqueous solution and industrial wastewater. *Journal of the Taiwan Institute of Chemical Engineers*. 2013;44:977-89.

[31] Katal R, Hasani E, Farnam M, Baei MS, Ghayyem MA. Charcoal ash as an adsorbent for Ni (II) adsorption and its application for wastewater treatment. *Journal of Chemical & Engineering Data*. 2012;57:374-83.

[32] Azizian S. Kinetic models of sorption: a theoretical analysis. *Journal of colloid and Interface Science*. 2004;276:47-52.

[33] Chen A-H, Liu S-C, Chen C-Y, Chen C-Y. Comparative adsorption of Cu (II), Zn (II), and Pb (II) ions in aqueous solution on the crosslinked chitosan with epichlorohydrin. *Journal of Hazardous materials*. 2008;154:184-91.

[34] Debbaudt A, Ferreira M, Gschaider M. Theoretical and experimental study of M<sup>2+</sup> adsorption on biopolymers. III. Comparative kinetic pattern of Pb, Hg and Cd. *Carbohydrate Polymers*. 2004;56:321-32.

[35] Genç Ö, Soysal L, Bayramoğlu G, Arıca M, Bektaş S. Procion Green H-4G immobilized poly (hydroxyethylmethacrylate/chitosan) composite membranes for heavy metal removal. *Journal of hazardous materials*. 2003;97:111-25.

[36] Sun S, Wang L, Wang A. Adsorption properties of crosslinked carboxymethyl-chitosan resin with Pb (II) as template ions. *Journal of hazardous materials*. 2006;136:930-7.

[37] Moradi O, Aghaie M, Zare K, Monajjemi M, Aghaie H. The study of adsorption characteristics Cu<sup>2+</sup> and Pb<sup>2+</sup> ions onto PHEMA and P (MMA-HEMA) surfaces from aqueous single solution. *Journal of hazardous materials*. 2009;170:673-9.

[38] Banerjee M, Basu RK, Das SK. Cu (II) removal using green adsorbents: kinetic modeling and plant scale-up design. *Environmental Science and Pollution Research*. 2018;1-16.

[39] Katal R, Baei MS, Rahmati HT, Esfandian H. Kinetic, isotherm and thermodynamic study of nitrate adsorption from aqueous solution using modified rice husk. *Journal of Industrial and Engineering Chemistry*. 2012;18:295-302.

